



ELSEVIER

Available online at www.sciencedirect.com

SCIENCE @ DIRECT®

Physics Letters B 561 (2003) 225–232

PHYSICS LETTERS B

www.elsevier.com/locate/npe

Study of hadronic five-body decays of charmed mesons

FOCUS Collaboration

J.M. Link^a, M. Reyes^a, P.M. Yager^a, J.C. Anjos^b, I. Bediaga^b, C. Göbel^b, J. Magnin^b,
A. Massafferri^b, J.M. de Miranda^b, I.M. Pepe^b, A.C. dos Reis^b, S. Carrillo^c,
E. Casimiro^c, E. Cuautle^c, A. Sánchez-Hernández^c, C. Uribe^c, F. Vázquez^c,
L. Agostino^d, L. Cinquini^d, J.P. Cumalat^d, B. O'Reilly^d, J.E. Ramirez^d, I. Segoni^{d,*},
M. Wahl^d, J.N. Butler^e, H.W.K. Cheung^e, G. Chiodini^e, I. Gaines^e, P.H. Garbincius^e,
L.A. Garren^e, E. Gottschalk^e, P.H. Kasper^e, A.E. Kreymer^e, R. Kutschke^e,
L. Benussi^f, S. Bianco^f, F.L. Fabbri^f, A. Zallo^f, C. Cawlfeld^g, D.Y. Kim^g,
A. Rahimi^g, J. Wiss^g, R. Gardner^h, A. Kryemadhi^h, C.H. Changⁱ, Y.S. Chungⁱ,
J.S. Kangⁱ, B.R. Koⁱ, J.W. Kwakⁱ, K.B. Leeⁱ, K. Cho^j, H. Park^j, G. Alimonti^k,
S. Barberis^k, M. Boschini^k, A. Cerutti^k, P. D'Angelo^k, M. DiCorato^k, P. Dini^k,
L. Edera^k, S. Erba^k, M. Giammarchi^k, P. Inzani^k, F. Leveraro^k, S. Malvezzi^k,
D. Menasce^k, M. Mezzadri^k, L. Milazzo^k, L. Moroni^k, D. Pedrini^k, C. Pontoglio^k,
F. Prelz^k, M. Rovere^k, S. Sala^k, T.F. Davenport III^l, V. Arena^m, G. Boca^m,
G. Bonomi^m, G. Gianini^m, G. Liguori^m, M.M. Merlo^m, D. Pantea^m, D.L. Pegna^m,
S.P. Ratti^m, C. Riccardi^m, P. Vitulo^m, H. Hernandezⁿ, A.M. Lopezⁿ, E. Luiggiⁿ,
H. Mendezⁿ, E. Montielⁿ, D. Olayaⁿ, A. Parisⁿ, J. Quinonesⁿ, W. Xiongⁿ, Y. Zhangⁿ,
J.R. Wilson^o, T. Handler^p, R. Mitchell^p, D. Engh^q, M. Hosack^q, W.E. Johns^q,
M. Nehring^q, P.D. Sheldon^q, K. Stenson^q, E.W. Vaandering^q, M. Webster^q, M. Sheaff^r

^a University of California, Davis, CA 95616, USA

^b Centro Brasileiro de Pesquisas Físicas, Rio de Janeiro RJ, Brazil

^c CINVESTAV, 07000 México City, DF, Mexico

^d University of Colorado, Boulder, CO 80309, USA

^e Fermi National Accelerator Laboratory, Batavia, IL 60510, USA

^f Laboratori Nazionali di Frascati dell'INFN, Frascati I-00044, Italy

^g University of Illinois, Urbana-Champaign, IL 61801, USA

^h Indiana University, Bloomington, IN 47405, USA

ⁱ Korea University, Seoul 136-701, South Korea

^j Kyungpook National University, Taegu 702-701, South Korea

^k INFN and University of Milano, Milano, Italy

^l University of North Carolina, Asheville, NC 28804, USA

^m Dipartimento di Fisica Nucleare e Teorica and INFN, Pavia, Italy

ⁿ University of Puerto Rico, Mayaguez, PR 00681, USA

^o University of South Carolina, Columbia, SC 29208, USA

^p University of Tennessee, Knoxville, TN 37996, USA

^q Vanderbilt University, Nashville, TN 37235, USA

^r University of Wisconsin, Madison, WI 53706, USA

Received 7 February 2003; received in revised form 27 March 2003; accepted 28 March 2003

Editor: L. Montanet

Abstract

We study the decay of D^+ and D_s^+ mesons into charged five-body final states, and report the discovery of the decay mode $D^+ \rightarrow K^+K^-\pi^+\pi^+\pi^-$, as well as measurements of the decay modes $D^+ \rightarrow K^-\pi^+\pi^+\pi^+\pi^-$, $D_s^+ \rightarrow K^+K^-\pi^+\pi^+\pi^-$, $D_s^+ \rightarrow \phi\pi^+\pi^+\pi^-$ and $D^+/D_s^+ \rightarrow \pi^+\pi^+\pi^+\pi^-\pi^-$. An analysis of the resonant substructure for $D^+ \rightarrow K^-\pi^+\pi^+\pi^+\pi^-$ and $D_s^+ \rightarrow K^+K^-\pi^+\pi^+\pi^-$ is included, with an indication that both decays proceed primarily through an a_1 vector resonance.

© 2003 Published by Elsevier Science B.V. Open access under [CC BY license](#).

PACS: 13.25.Ft; 14.40.Lb

The hadronic five-body decays of charmed mesons have been studied in recent years [1–6], but limited statistics have prevented precise measurements of their resonant substructure. Theoretical predictions are limited mainly to two-body decay modes, and little is known about how five-body final states are produced. Theoretical discussion suggests a “vector-dominance model”, in which heavy flavor mesons decay into a two-body intermediate state by emitting a W , which immediately hadronizes into a charged vector, axial vector, or pseudoscalar meson [7]. The charged meson then decays strongly to produce a many-body final state. In this model five-body final states arise from the axial vector meson, $a_1(1260)^+$, which decays into three pions, and a second resonance which decays to two bodies.

The FOCUS Collaboration [8–10] has studied two five-body decay modes, $D^+ \rightarrow K^-\pi^+\pi^+\pi^+\pi^-$ and $D_s^+ \rightarrow K^+K^-\pi^+\pi^+\pi^-$. There is an indication that the resonant substructure in both modes is dominated by a two-body vector resonance involving the $a_1(1260)^+$. We also present inclusive branching ratio measurements of four charged five-body hadronic de-

cays, including the first evidence of the decay mode $D^+ \rightarrow K^+K^-\pi^+\pi^+\pi^-$.

Five-body D^+ and D_s^+ decays are reconstructed using a candidate driven vertex algorithm [8]. A decay vertex is formed from the five reconstructed tracks. The momentum vector of the parent D meson is then used as a seed to intersect other tracks in order to find the production vertex. Events are selected based on several criteria. The confidence level of the decay vertex must be greater than 1%. The confidence level that a track from the decay vertex intersects the production vertex must be less than 1%. The likelihood for each particle to be a proton, kaon, pion, or electron based on Čerenkov particle identification is used to make additional requirements [9]. For each kaon candidate we require the negative log-likelihood kaon hypothesis, $W_K = -2 \ln(\text{kaon likelihood})$, to be favored over the corresponding pion hypothesis W_π by $W_\pi - W_K > 3$. In addition, for each pion candidate we require the pion hypothesis to be favored over any alternative hypothesis. We also require the significance of separation of the production and decay vertices to be at least 10. In order to reduce background due to secondary interactions of particles from the production vertex, we require the D reconstructed momentum to be greater than 25 GeV/ c and the secondary vertex to be located outside of the target material. Finally,

* Corresponding author.

E-mail address: segoni@pizero.colorado.edu (I. Segoni).

URL address: <http://www-focus.fnal.gov/authors.html>.

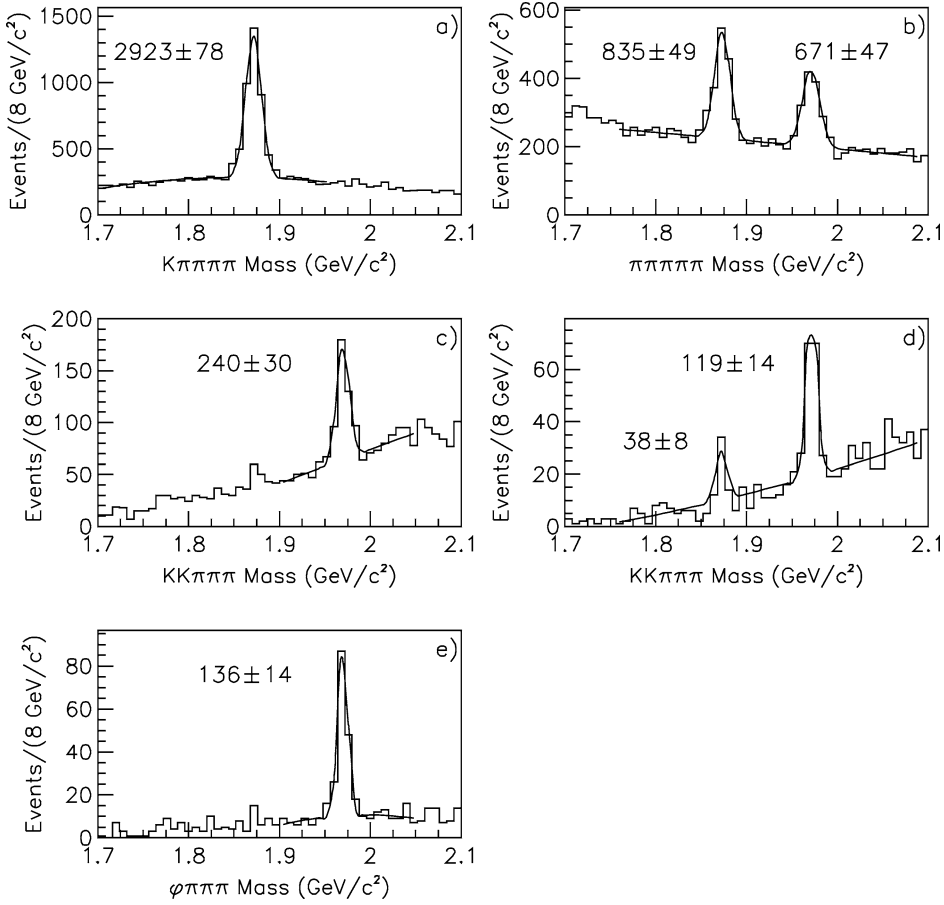


Fig. 1. (a) $K4\pi$ invariant mass distribution. (b) 5π invariant mass distribution. (c) $KK3\pi$ invariant mass distribution for D_s^+ optimized cuts. (d) $KK3\pi$ invariant mass distribution for D^+ optimized cuts. (e) $\phi3\pi$ invariant mass distribution. The fits are described in the text and the numbers quoted are the yields.

we remove events that are consistent with various D^* decays.

We turn to additional analysis cuts made in individual modes, beginning with $D^+ \rightarrow K^-\pi^+\pi^+\pi^-\pi^-$. Because this mode is the most abundant we apply only the standard cuts already discussed. Fig. 1(a) shows the $K4\pi$ invariant mass plot. The distribution is fitted with a Gaussian for the D^+ signal and a 2nd degree polynomial for the background. A binned maximum likelihood fit gives 2923 ± 78 events.

The $D^+/D_s^+ \rightarrow \pi^+\pi^+\pi^+\pi^-\pi^-$ modes are more difficult to detect, due to the large combinatorial background. To reduce this background we increase the separation of the secondary vertex from being just outside the target material to two standard deviations from the edge of the target material. We remove

the decays $D^+/D_s^+ \rightarrow \eta'\pi^+$, $\eta' \rightarrow \pi^+\pi^+\pi^-\pi^-$ by requiring the four pion reconstructed mass to be larger than the $\eta' - \pi^0$ mass difference, that is, $M_{4\pi} > 0.825 \text{ GeV}/c^2$. Fig. 1(b) shows the five-pion invariant mass plot for events that satisfy these cuts. The distribution is fitted with a Gaussian for the D^+ signal (835 ± 49 events), another Gaussian for the D_s^+ signal (671 ± 47 events) and a 1st degree polynomial for the background.

For the $D_s^+ \rightarrow K^+K^-\pi^+\pi^+\pi^-$ mode the requirement of two kaons in the final state greatly reduces background, allowing us to apply only the standard cuts used in all modes. Fig. 1(c) shows the $KK3\pi$ invariant mass plot for events satisfying these cuts. We fit to a Gaussian (240 ± 30 events) and 2nd degree polynomial.

Table 1

Branching ratios for five-body modes and comparison to the previous measurements by E687. All branching ratios are inclusive of subresonant modes

Decay mode	FOCUS	E687 [6]
$\frac{\Gamma(D^+ \rightarrow K^- \pi^+ \pi^+ \pi^+ \pi^-)}{\Gamma(D^+ \rightarrow K^- \pi^+ \pi^+)}$	$0.058 \pm 0.002 \pm 0.006$	$0.077 \pm 0.008 \pm 0.010$
$\frac{\Gamma(D^+ \rightarrow \pi^+ \pi^+ \pi^+ \pi^- \pi^-)}{\Gamma(D^+ \rightarrow K^- \pi^+ \pi^+ \pi^+ \pi^-)}$	$0.290 \pm 0.017 \pm 0.011$	$0.299 \pm 0.061 \pm 0.026$
$\frac{\Gamma(D_s^+ \rightarrow \pi^+ \pi^+ \pi^+ \pi^- \pi^-)}{\Gamma(D_s^+ \rightarrow K^- K^+ \pi^+)}$	$0.145 \pm 0.011 \pm 0.010$	$0.158 \pm 0.042 \pm 0.031$
$\frac{\Gamma(D_s^+ \rightarrow K^+ K^- \pi^+ \pi^+ \pi^-)}{\Gamma(D_s^+ \rightarrow K^- K^+ \pi^+)}$	$0.150 \pm 0.019 \pm 0.025$	$0.188 \pm 0.036 \pm 0.040$
$\frac{\Gamma(D_s^+ \rightarrow \phi \pi^+ \pi^+ \pi^-)}{\Gamma(D_s^+ \rightarrow \phi \pi^+)}$	$0.249 \pm 0.024 \pm 0.021$	$0.28 \pm 0.06 \pm 0.01$
$\frac{\Gamma(D^+ \rightarrow K^+ K^- \pi^+ \pi^+ \pi^-)}{\Gamma(D^+ \rightarrow K^- \pi^+ \pi^+ \pi^+ \pi^-)}$	$0.040 \pm 0.009 \pm 0.019$	

For the $K^+ K^- \pi^+ \pi^+ \pi^-$ final state we have also studied the subresonant decay $D_s^+ \rightarrow \phi \pi^+ \pi^+ \pi^-$, by additionally requiring the $K^+ K^-$ invariant mass combination to be consistent with the ϕ mass. The $\phi \pi^+ \pi^+ \pi^-$ invariant mass plot is shown in Fig. 1(e). We fit to a Gaussian (136 ± 14 events) and 2nd degree polynomial.

The decay $D^+ \rightarrow K^+ K^- \pi^+ \pi^+ \pi^-$ is Cabibbo suppressed. We require a significance of vertex separation of 20, a reconstructed D^+ momentum of greater than $50 \text{ GeV}/c$, and tighten particle identification cuts on both kaons to $W_\pi - W_K > 4$. Fig. 1(d) shows the resulting $K^+ K^- \pi^+ \pi^+ \pi^-$ invariant mass plot. This is the first observation of this mode. We fit with a Gaussian for the D^+ signal (38 ± 8 events), another Gaussian for the D_s events and a 2nd degree polynomial for the background.

We measure the branching fraction of the $D^+ \rightarrow K^- \pi^+ \pi^+ \pi^+ \pi^-$ mode relative to $D^+ \rightarrow K^- \pi^+ \pi^+$, then measure the branching fractions of the other D^+ modes relative to the $D^+ \rightarrow K^- \pi^+ \pi^+ \pi^+ \pi^-$ to reduce systematic effects due to differences in the number of decay products. All D_s^+ decay modes are measured relative to $D_s^+ \rightarrow K^+ K^- \pi^+$. For modes included in our resonant substructure analysis the Monte Carlo simulation contains the incoherent mixture of subresonant decays determined by our analysis. For modes not included in our resonant substructure analyses, the Monte Carlo is composed of five-body phase space. We test for dependency on cut selection by individually varying each cut. The results, compared with existing measurements, are shown in Table 1.

We studied systematic effects due to uncertainties in the reconstruction efficiency, in the unknown reso-

nant substructure, and on the fitting procedure. To determine the systematic error due the reconstruction efficiency we follow a procedure based on the S-factor method used by the Particle Data Group [11]. For each mode we split the data sample into four independent subsamples based on D momentum and period of time in which the data was collected. These splits provide a check on the Monte Carlo simulation of charm production, of the vertex detector (it changed during the course of the run), and on the simulation of the detector stability. We then define the split sample variance as the difference between the scaled variance and the statistical variance if the scaled variance exceeds the statistical variance. To determine the systematic effects associated with the Monte Carlo simulation of multi-body decays, the branching ratios are evaluated by varying the isolation of the production vertex, with the variance used as the systematic error. We also varied the mixtures of subresonant states in the Monte Carlo and used the variance in the branching ratios as a contribution to the systematic error. We also determine the systematic effects based on different fitting procedures. The branching ratios are evaluated under various fit conditions, and the variance is used as the systematic error, as all fit variants are a priori equally likely. Finally, we evaluate systematic effects from uncertainty in absolute tracking efficiency of multi-body decays using studies of $D^0 \rightarrow K^- \pi^+ \pi^+ \pi^-$ and $D^0 \rightarrow K^- \pi^+$ decays. The systematic effects are then all added together in quadrature to obtain the final systematic error.

In addition to reporting inclusive branching ratio measurements, we have studied the resonance substructure in two decays: $D^+ \rightarrow K^- \pi^+ \pi^+ \pi^+ \pi^-$

and $D_s^+ \rightarrow K^+K^-\pi^+\pi^+\pi^-$. We use an incoherent binned fit method which assumes the final state is an incoherent superposition of subresonant decay modes containing vector resonances. A coherent analysis would be difficult given the statistics of this experiment. For the $D^+ \rightarrow K^-\pi^+\pi^+\pi^+\pi^-$ mode we consider the lowest mass ($K^-\pi^+$) and ($\pi^+\pi^-$) resonances, as well as a nonresonant channel: $\overline{K}^{*0}\pi^-\pi^+\pi^+$, $K^-\rho^0\pi^+\pi^+$, $\overline{K}^{*0}\rho^0\pi^+$, and $(K^-\pi^+\pi^+\pi^-\)_{NR}. All states not explicitly considered are assumed to be included in the nonresonant channel.$

We determine the acceptance corrected yield into each subresonant mode using a technique whereby each event is weighted by its values in three submasses: ($K^-\pi^+$), ($\pi^+\pi^-$), and ($\pi^+\pi^+$). No resonance in the ($\pi^+\pi^+$) submass exists, but we include it in order to compute a meaningful χ^2 estimate of the fit. Eight population bins are constructed depending on whether each of the three submasses falls within the expected resonance. (In the case of $\pi^+\pi^+$, the bin is split into high and low mass regions.) For each Monte Carlo simulation the bin population, n_i , in the eight bins is determined and a transport matrix, $T_{i\alpha}$, is calculated between the generated states, α , Monte Carlo yields, Y_α , and the eight bins i .

$$n_i = \sum_{\alpha} T_{i\alpha} Y_{\alpha}.$$

The elements of the transport matrix, T , can be summed to give the efficiency for each mode, ϵ_{α}

$$\epsilon_{\alpha} = \sum_i T_{i\alpha}.$$

The Monte Carlo determined transport matrix is inverted to create a new density matrix which multiplies the bin populations to produce corrected yields. The density weight includes the contributions from the twelve combinations we have for each event. Each data event can then be weighted according to its values in the submass bins. Once the weighted distributions for each of the four modes are generated, we determine the acceptance corrected yield by fitting the distributions with a Gaussian signal and a linear background. Using incoherent Monte Carlo mixtures of the four subresonant modes we verified that our procedure was able to correctly recover the generated mixtures of the four modes.

Table 2

Fractions relative to the inclusive mode and comparison to previous measurements for the resonance substructure of the $D^+ \rightarrow K^-\pi^+\pi^+\pi^+\pi^-$ decay mode. These values are not corrected for unseen decay modes

Subresonant mode	Fraction of $K4\pi$	E687 fraction [6]
$(K^-\pi^+\pi^+\pi^+\pi^-)_{NR}$	$0.07 \pm 0.05 \pm 0.01$	< 0.26 (90% C.L.)
$\overline{K}^{*0}\pi^-\pi^+\pi^+$	$0.21 \pm 0.04 \pm 0.06$	0.42 ± 0.14
$K^-\rho^0\pi^+\pi^+$	$0.30 \pm 0.04 \pm 0.01$	0.44 ± 0.14
$\overline{K}^{*0}\rho^0\pi^+$	$0.40 \pm 0.03 \pm 0.06$	0.20 ± 0.09

The results for $K^-\pi^+\pi^+\pi^+\pi^-$ are summarized and compared to the E687 results in Table 2. Taking into account the correlation among the subresonant fractions, the calculated χ^2 for the hypothesis that the results are consistent with E687 is 6.5 (4 degrees of freedom). The four weighted histograms with fits are shown in Fig. 2. Fig. 2(e) is the weighted distribution for the sum of all subresonant modes. The goodness of fit is evaluated by calculating a χ^2 for the hypothesis of consistency between the model predictions and observed data yields in each of the 8 submass bins. The calculated χ^2 is 7.4 (4 degrees of freedom), with most of the χ^2 contribution resulting from a poor Monte Carlo simulation of the $\pi^+\pi^+$ spectrum for the $\overline{K}^{*0}\rho^0\pi^+$ mode. We assessed systematic errors by individually varying the width of the submass bins corresponding to the ρ and \overline{K}^{*0} resonances by 20%. The systematic error is then estimated as the variance of the two measurements with varied widths, along with the original measurement. Since our methods of calculating subresonant fractions and inclusive branching ratios are distinct, statistical and systematic errors are added in quadrature when normalizing our subresonant fractions to other modes.

We follow a similar procedure for the $D_s^+ \rightarrow K^+K^-\pi^+\pi^+\pi^-$, treating the final state as an incoherent superposition of the (K^+K^-) and ($\pi^+\pi^-$) resonances, as well as a nonresonant channel: $\phi\pi^+\pi^+\pi^-$, $K^+K^-\rho\pi^+$, $\phi\rho\pi^+$ and $(K^+K^-\pi^+\pi^+\pi^-)_{NR}$. Each event is weighted by its value in each of three submasses: (K^+K^-), ($\pi^+\pi^-$), and ($\pi^+\pi^+$), and the weighted distributions are again fitted with a Gaussian signal and a linear background. The results are summarized in Table 3 and are presented in Fig. 3. The goodness of fit is evaluated by calculating a χ^2 for the hypothesis of consistency between the model pre-

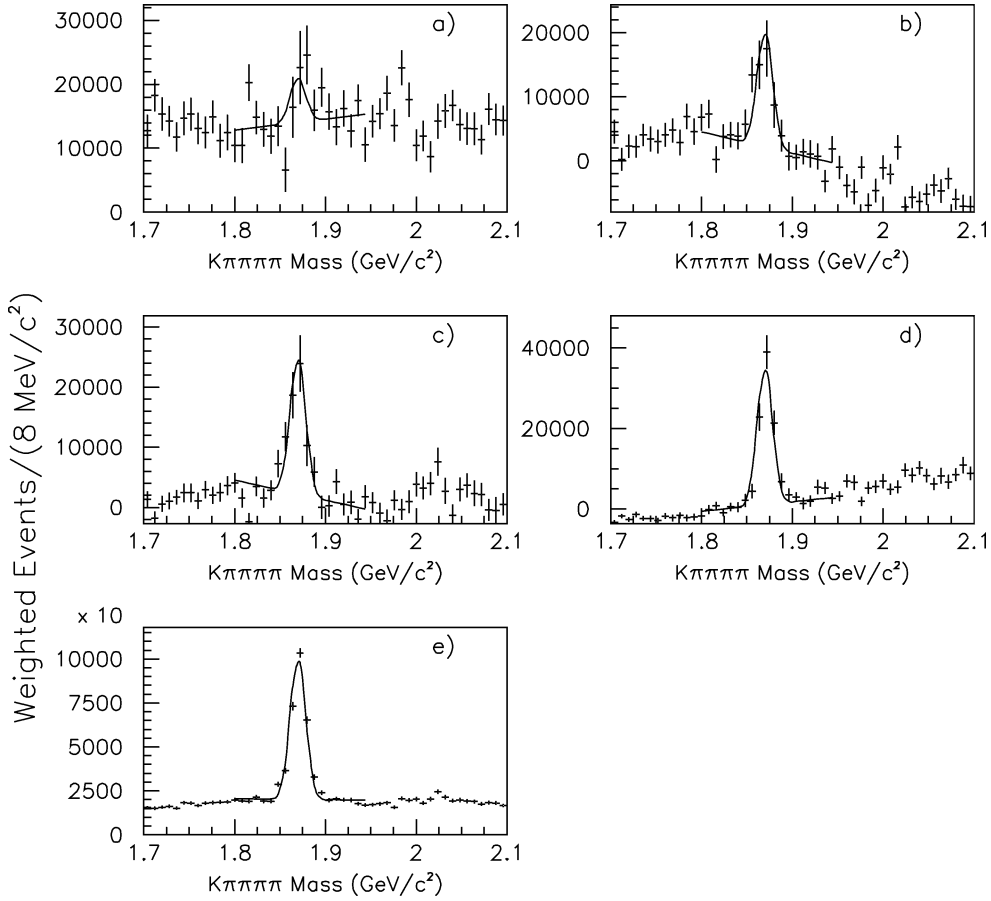


Fig. 2. $K^-\pi^+\pi^+\pi^+\pi^-$ weighted invariant mass for (a) $(K^-\pi^+\pi^+\pi^+\pi^-)_{\text{NR}}$, (b) $\overline{K}^{*0}\pi^-\pi^+\pi^+$, (c) $K^-\rho^0\pi^+\pi^+$, (d) $\overline{K}^{*0}\rho^0\pi^+$, (e) inclusive sum of all four modes.

dictions and observed data yields in each of the eight submass bins. The calculated χ^2 is 10.2 (4 degrees of freedom), with most of the χ^2 contribution resulting from a poor Monte Carlo simulation of the $\pi^+\pi^+$ spectrum in the nonresonant channel. We assess systematic errors by calculating the variance of our results with 20% variations in the width of the submass bins corresponding to the ρ and ϕ resonances.

In both resonant substructure analyses the dominant mode is of the form vector–vector–pseudoscalar: $\overline{K}^{*0}\rho^0\pi^+$ and $\phi\rho^0\pi^+$ in the case of $K^-\pi^+\pi^+\pi^+\pi^-$ and $K^+K^-\pi^+\pi^+\pi^-$, respectively. Given the phase space constraints for both of these decays, such a result is unexpected. However, theoretical discussion of a vector-dominance model for heavy flavor decays [7] suggests that charm decays are dominated by

Table 3

Fractions relative to the inclusive mode for the resonance substructure of the $D_s^+ \rightarrow K^+K^-\pi^+\pi^+\pi^-$ decay mode. These values are not corrected for unseen decay modes

Subresonant mode	Fraction of $2K3\pi$
$(K^+K^-\pi^+\pi^+\pi^-)_{\text{NR}}$	$0.10 \pm 0.06 \pm 0.05$
$\phi\pi^-\pi^+\pi^+$	$0.21 \pm 0.05 \pm 0.06$
$K^+K^-\rho^0\pi^+$	< 0.03 (90% C.L.)
$\phi\rho^0\pi^+$	$0.75 \pm 0.06 \pm 0.04$

quasi-two-body decays in which the W^\pm immediately hadronizes into a charged pseudoscalar, vector, or axial vector meson. Thus branching ratios of the form $D \rightarrow a_1(1260)^+X$ are of comparable value to those observed for $D \rightarrow \pi^+X$, when adjusted for phase space. Such theoretical discussion raises the possi-

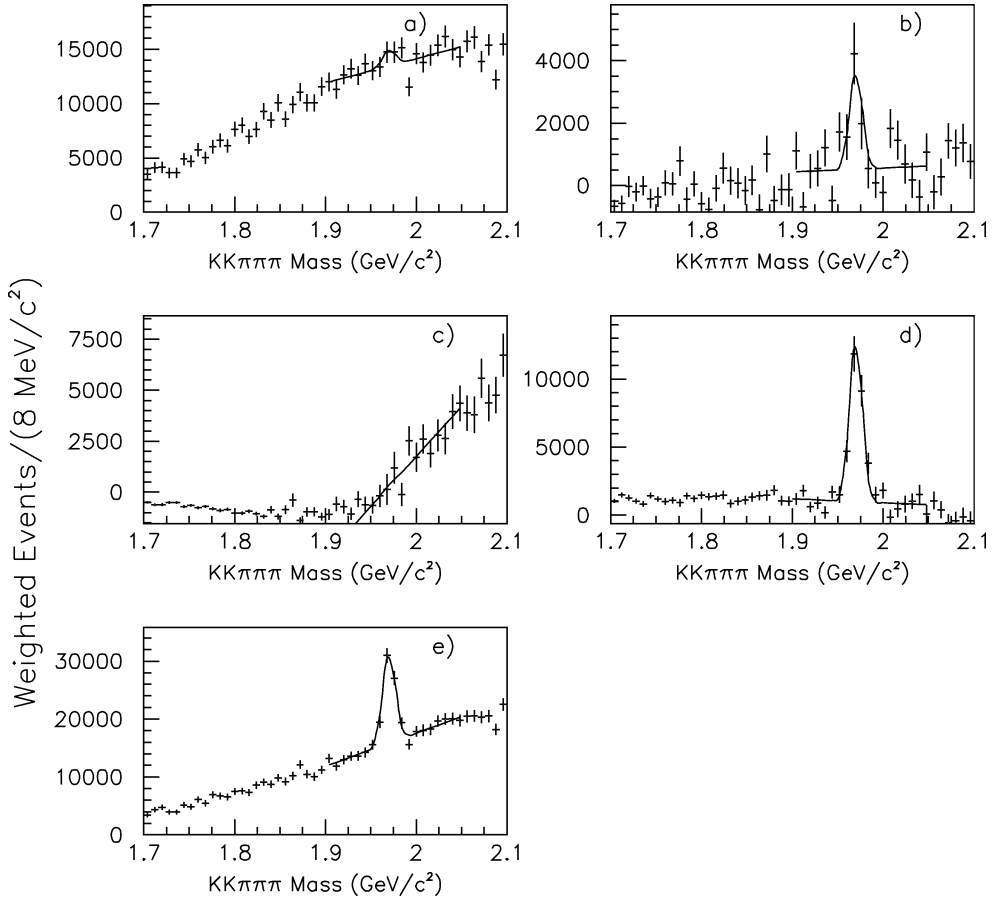


Fig. 3. $K^+K^-\pi^+\pi^+\pi^-$ weighted invariant mass for (a) $(K^+K^-\pi^+\pi^+\pi^-)_{NR}$, (b) $\phi\pi^-\pi^+\pi^+$, (c) $K^+K^-\rho^0\pi^+$, (d) $\phi\rho^0\pi^+$, (e) inclusive sum of all four modes.

bility that the resonant substructure for both modes is dominated by a quasi-two-body decay involving the a_1 : $\overline{K}^{*0}a_1^+$ and ϕa_1^+ for $K^-\pi^+\pi^+\pi^+\pi^-$ and $K^+K^-\pi^+\pi^+\pi^-$, respectively, where $a_1^+ \rightarrow \rho^0\pi^+$. Although the central value of the a_1 mass lies outside of phase space for both decays, these decay modes are allowed due to the large width of the a_1 . However, the large width of the a_1 and its position in phase space make the resonance difficult to detect directly.

To verify the hypothesis that subresonant decays are proceeding through a_1 we generate Monte Carlo simulations of $D^+ \rightarrow \overline{K}^{*0}a_1^+$ and $D_s^+ \rightarrow \phi a_1^+$, assuming the a_1 has a width of 400 MeV/ c^2 and decays entirely as an S-wave, and use our subresonant analysis procedure explained above. We compare the event

yield fractions in each subresonant mode obtained on data with those obtained by the Monte Carlo. We calculate branching ratios for the decays $D^+ \rightarrow \overline{K}^{*0}a_1^+$ and $D_s^+ \rightarrow \phi a_1^+$ using the ratios of the largest observed fractions of $K^{*0}\rho\pi^+$ and $\phi\rho\pi$ from data (40% and 75%) to those observed from Monte Carlo simulations of $D^+ \rightarrow \overline{K}^{*0}a_1^+$ and $D_s^+ \rightarrow \phi a_1^+$ (70% and 78%). Assuming the a_1^+ branching fraction to $\rho^0\pi^+$ is 50% and correcting for the Particle Data Group ϕ and K^{*0} branching fractions [11], the $D^+ \rightarrow \overline{K}^{*0}a_1^+$ and $D_s^+ \rightarrow \phi a_1^+$ branching fractions, including unseen decays, are shown in Table 4. We assess systematic errors by increasing the width of the a_1 resonance in our generated Monte Carlo to 600 MeV/ c^2 , taking the systematic error as the variance of our measurements with the two widths.

Table 4

Inclusive branching ratios for a_1^+ states. These values are corrected for unseen decay modes

Decay mode	Fraction
$\frac{\Gamma(D^+ \rightarrow \overline{K^{*0}} a_1^+)}{\Gamma(D^+ \rightarrow K^- \pi^+ \pi^+)}$	$0.099 \pm 0.008 \pm 0.018$
$\frac{\Gamma(D_s^+ \rightarrow \phi a_1^+)}{\Gamma(D_s^+ \rightarrow K^+ K^- \pi^+)}$	$0.559 \pm 0.078 \pm 0.044$

In conclusion we have measured the relative branching ratios of five-body and three-body charged hadronic decays of D^+ and D_s^+ and have presented the first evidence of the decay mode $D^+ \rightarrow K^+ K^- \pi^+ \pi^+ \pi^-$. We have also performed an analysis of the resonant substructure in the decays $D^+ \rightarrow K^- \pi^+ \pi^+ \pi^+ \pi^-$ and $D_s^+ \rightarrow K^+ K^- \pi^+ \pi^+ \pi^-$. There is an indication that both decays proceed through a quasi-two-body decay involving the $a_1(1260)^+$ particle.

Acknowledgements

We acknowledge the assistance of the staffs of Fermi National Accelerator Laboratory, the INFN of Italy, and the physics departments of the collaborat-

ing institutions. This research was supported in part by the US National Science Foundation, the US Department of Energy, the Italian Istituto Nazionale di Fisica Nucleare and Ministero della Istruzione, Università e Ricerca, the Brazilian Conselho Nacional de Desenvolvimento Científico e Tecnológico, CONACyT-México, and the Korea Research Foundation of the Korean Ministry of Education.

References

- [1] H. Albrecht, et al., Phys. Lett. B 153 (1985) 343.
- [2] J.C. Anjos, et al., Phys. Rev. Lett. 60 (1988) 897.
- [3] P.L. Frabetti, et al., Phys. Lett. B 281 (1992) 167.
- [4] J.C. Anjos, et al., Phys. Rev. D 42 (1990) 2414.
- [5] S. Barlag, et al., E687 Collaboration, Z. Phys. C 55 (1992) 383.
- [6] P.L. Frabetti, et al., E687 Collaboration, Phys. Lett. B 401 (1997) 131.
- [7] H.J. Lipkin, Phys. Lett. B 515 (2001) 81.
- [8] P.L. Frabetti, et al., E687 Collaboration, Nucl. Instrum. Methods A 320 (1992) 519.
- [9] J.M. Link, et al., FOCUS Collaboration, Nucl. Instrum. Methods A 484 (2002) 270.
- [10] J.M. Link, et al., FOCUS Collaboration, hep-ex/0204023.
- [11] K. Hagiwara, et al., Particle Data Group, Phys. Rev. D 66 (2002) 010001.